Optimization of limit of detection in Taylor dispersion analysis: Application to the size determination of vaccine antigens

Camille Malburet, Michel Martin, Laurent Leclercq, Jean-François Cotte, Jérôme Thiebaud, Jean-Philippe Biron, Joseph Chamieh, Hervé Cottet

Optimization of limit of detection in Taylor Dispersion Analysis: application to the size determination of vaccine antigens

Camille Malburet[1,2], Michel Martin[3], Laurent Leclercq[1], Jean-François Cotte[2], Jérôme Thiebaud[2], Jean-Philippe Biron[1], Joseph Chamieh[1], Hervé Cottet[1*]

[1] IBMM, University of Montpellier, CNRS, ENSCM, Montpellier, France

[2] Sanofi, Analytical Sciences, 1541 avenue Marcel Mérieux, 69280 Marcy l'Etoile, France

[3] PMMH, CNRS, ESPCI Paris − PSL, Sorbonne Université, Université Paris Cité, Paris 75005, France

*Correspondence should be addressed to H.C (herve.cottet@umontpellier.fr). Full address: Institut des Biomolécules Max Mousseron, Bâtiment Balard, Pièce N3J17, 1919, Route de Mende, F-34293 Montpellier Cedex. Phone: +33 688167297.

Abstract

The development of a new vaccine requires the precise characterization of all the physicochemical parameters of the vaccine antigens, which are the molecules that induce the immune response. Taylor dispersion analysis (TDA) is a promising alternative technique for the determination of diffusion coefficients and hydrodynamic radii of proteins, macromolecules and nanoparticles. In this work, TDA was used to determine the hydrodynamic radius distribution and its average value of four antigens: diphtheria toxoid (DT), tetanus toxoid (TT), hepatitis B surface antigen (HBsAg) and polyribosyl-ribitol phosphate conjugated to tetanus toxoid (PRP-T). The robustness of the results obtained was investigated on bare fused silica capillary and hydroxypropylcellulose coated capillary. The impact of operational parameters on the limit of

detection (LOD) and limit of quantification (LOQ) were studied from both theoretical and experimental points of view. The influence of the diameter and the length of the capillary on the LOD and LOQ were studied as well as the impact of the mobilization pressure. General guidelines for the choice of the initial operating conditions are given for the development of future TDA methods.

Keywords: Taylor dispersion analysis, proteins, vaccines, limit of detection, limit of quantification, quantitative analysis.

1. Introduction

Taylor Dispersion Analysis (TDA) is a straightforward method for the determination of the diffusion coefficient and, thus, the hydrodynamic radius of nano-objects. TDA is based on the dispersion of a solute plug in an open tube under a laminar Poiseuille flow.[1,2] The dispersion is due to the combined action of the dispersive parabolic velocity profile and the molecular diffusion that redistributes the molecules in the cross-section of the capillary. When the conditions of validity of Taylor dispersion are fulfilled, the elution profile recorded as a function of time for a monomolecular sample is a Gaussian peak.[3] The determination of the temporal variance of the elution profile σ_t^2 allows to directly calculate the molecular diffusion coefficient D_m and the average hydrodynamic radius R_h by using the Stokes-Einstein equation. TDA can also provide both the individual hydrodynamic radius R_h and the relative amounts of a mixture of two or three analytes.[4–6] It can thus be considered as a separation method for which the selectivity is based on dispersion rather than on retention. Moreover, an original approach for the data analysis of polydisperse samples, based on Constrained Regularized Linear Inversion (CRLI), allows to obtain the size distribution of the nano-objects from the experimental taylorgrams.[7]

TDA does not require any calibration and the knowledge of the sample concentration is not needed for the size determination. Moreover, it is suitable for the analysis of low-abundant samples, as the injected volume is very small (only a few nL are typically injected). TDA is applicable to samples of different natures (small molecules[8], proteins[9], polymers[10], liposomes[11], microemulsions[12,13]), either in aqueous or nonaqueous liquid phases, with hydrodynamic radius (R_h) from 0.1 nm to about 150 nm.[14] This method has also recently shown promise for the study of vaccine antigens[15] and lipid nanoparticles for mRNA delivery.[16]

Vaccines have shown their effectiveness throughout history on the occurrence of infectious diseases.[17,18] In addition to preventing deaths, vaccines also massively reduce complications and disabilities.[19] Yet many diseases still lack effective treatment and new epidemics are frequently emerging.[20] Furthermore, vaccines have today the potential to prevent or treat different types of diseases such as cancer[21] and neurodegenerative disorders[22]. In vaccines' products, antigens are the substances that trigger the immune response. The development of a new vaccine, and the release of commercial lots, requires characterizing the physicochemical properties of antigens in details, including their size.

The first part of this work was focused on the development of a method allowing to characterize the size of four vaccine antigens: two toxoids, namely diphtheria toxoid (DT) against diphtheria and tetanus toxoid (TT) against tetanus, a subviral particle named Hepatitis B surface Antigen (HBsAg) for the prevention of *Hepatitis B* infection and a glycoconjugate named polyribosyl-ribitol phosphate conjugated to tetanus toxoid (PRP-T) for the prevention of *Haemophilus influenzae type b* infection.

As antigens are often at low concentrations in vaccine formulations, the limit of detection (LOD) of the TDA method should be as low as possible. The second part of this work aims at finding the optimal conditions to obtain the lowest LOD in TDA. Three main operating parameters, namely the capillary radius, the applied pressure and the capillary total length were studied for the optimization.

2. Material and methods

2.1. Chemicals and Materials. Diphtheria toxoid (DT) and tetanus toxoid (TT) were provided at 18.5 g/L and 20.7 g/L in a 10 mM PBS, 200 mM glycine and 154 mM NaCl mixture buffered at pH 6.9 by Sanofi (Marcy-l'Étoile, France). Hepatitis B surface antigen (HBsAg) was provided at 1.6 g/L in a 10 mM PBS and 154 mM NaCl mixture buffered at pH 7.4 by Sanofi (Marcy-l'Étoile, France). Polyribosyl-ribitol phosphate conjugated to tetanus toxoid (PRP-T) was provided at 0.56 g/L in a 10 mM TRIS and 8% (w/w) sucrose mixture buffered at pH 7.4 by Sanofi (Marcy-l'Étoile, France). Tris(hydroxymethyl)aminomethane (TRIS, $(CH_2OH)_3CNH_2$, M_w = 121 g/mol), Phosphate-Buffered Saline tablets (PBS), glycine (NH_2CH_2COOH, M_w = 75.07 g/mol), sucrose ($C_{12}H_{22}O_{11}$, M_w = 342.30 g/mol) and hydroxypropyl cellulose (HPC, $M_w = 1 \times 10^5$ g/mol) were purchased from Merk (Darmstadt, Germany). Bare fused silica capillaries were purchased from Molex Polymicro Technologies (Phoenix, USA). Deionized water was further purified with a Milli-Q system from Millipore (Molsheim, France).

2.2. Sample preparation. Stock solutions of DT, TT, HBsAg and PRP-T were diluted to 0.4 g/L in their respective analytical buffer. HBsAg was further diluted until 0.01 g/L in its analytical buffer. Final solutions were homogenized by manual stirring before analysis.

2.3. Capillary coating. HPC capillaries coatings were performed based on a previously published protocol.[23] Bare fused silica capillaries of 75 µm i.d. × 75 cm total length (66.5 cm to the detector) were used. HPC was dissolved in water at room temperature to 5% (w/w) final concentration. The capillaries were flushed 30 min at 1 bar with the polymer solution using capillary electrophoresis equipment and then heated in a gas chromatography oven (GC-14 A, Shimadzu, France) under a nitrogen stream of 30 kPa. Temperature program was: 60°C for 10 min, then 5°C/min gradient from 60°C to 140°C and finally, 140°C for 20 min. Before use and between

two samples, the coated capillaries were rinsed 2 min with water and then 2 min with the analysis buffer at 1 bar.

2.4. Taylor Dispersion Analysis (TDA). All experiments were carried out on a 1600 CE Agilent system (Santa Clara, USA). This system is equipped with a diode array detector (DAD). Capillaries dimensions and injections conditions are stated in each figure caption. The elution peaks obtained by TDA were fitted by the sum of Gaussians, according to equation (1) using a home-developed Excel spreadsheet:

$$S(t) = \sum_{i=1}^{2} \frac{A_i}{\sigma_{t,i}\sqrt{2\pi}} \exp\left[-\frac{(t-t_0)^2}{2\sigma_{t,i}^2} \right] \quad (1)$$

where $S(t)$ is the absorbance signal, $\sigma_{t,i}^2$ is the temporal variance, A_i is a constant that depended on the response factor and the injected quantity of solute and t_0 is the average elution time. t_0 is directly obtained from the position of the maximum of absorbance and σ_i, and A_i are adjusting parameters obtained by nonlinear least square regression using Excel solver.

The temporal variance $\sigma_{t,i}^2$ allows to calculate the molecular diffusion coefficient $D_{m,i}$ according to equation (2):

$$D_{m,i} = \frac{R_c^2 t_0}{24\sigma_{t,i}^2} \quad (2)$$

where R_c is the capillary radius. Stokes–Einstein equation (3) allows then to determine the hydrodynamic radius $R_{h,i}$:

$$R_{h,i} = \frac{k_B T}{6\pi\eta D_{m,i}} \quad (3)$$

where k_B is the Boltzmann constant, T is the temperature, and η is the eluent viscosity.

The validity of TDA and equation (2) is conditioned to the assessment of two requirements.[3] First, the axial (longitudinal) diffusion must be negligible compared to the dispersion due to the parabolic velocity profile. Second, the average elution time must be longer than the characteristic time of diffusion of the analyte in the cross section of the capillary. For a relative error on the determination of the molecular diffusion coefficient (D_m) lower than 3%[24], the two conditions lead to equations (4) and (5):

$$P_e = \frac{u\,R_c}{D_m} \geq 40 \qquad (4)$$

were P_e is the Péclet number and u is the linear mobile phase velocity.

$$\tau = \frac{D_m\,t_0}{R_c^2} \geq 1.25 \qquad (5)$$

where τ is an adimensional parameter inversely proportional to the characteristic time of diffusion across the capillary section.

To get the size distribution, the elution profile was fitted using a second approach based on the Constrained Regularized Linear Inversion (CRLI) algorithm[7] according to equation (6):

$$S(t) = \int_0^\infty CM(D_m)\,\rho(D_m)\sqrt{D_m}\,\exp\left[-\frac{12(t-t_0)^2\,D_m}{R_c^2 t_0}\right] dD_m \qquad (6)$$

where C is an instrumental constant, $M(D_m)$ and $\rho(D_m)$ are the molar mass and the molar concentration in the injected sample of the objects with the diffusion coefficient D_m, respectively.

2.5. Calculation of the limit of detection (LOD) and limit of quantification (LOQ).

The LOD was calculated according to equation (7):

$$LOD = \frac{3G}{a} \qquad (7)$$

where G is the standard deviation of the blank signals and a is the slope of the calibration curve, *i.e.* the plot of the peak height *vs.* the analyte concentration in the injected sample, in given operating conditions.

In the same way the LOQ was determined according to equation (8):

$$LOQ = \frac{10G}{a} \tag{8}$$

3. Theoretical background

3.1. Optimization of the limit of detection (LOD) in TDA. In the following, we assume that the taylorgram of a single analyte has a Gaussian shape:

$$S(t) = S_0 \exp\left[-\frac{(t-t_0)^2}{2\sigma_t^2}\right] \tag{9}$$

where S is the detector signal at time t, S_0 the maximum value of the signal at the average analyte elution time t_0 and σ_t the temporal standard deviation of the signal. As the detector is assumed to provide a signal proportional to the concentration, c, of the analyte in the detector, then:

$$S(t) = k\,c(t) \tag{10}$$

where k is the detector response factor for the analyte. Let m be the amount of analyte injected in the capillary. As in TDA, the whole injected analyte is flowing through the detector, m becomes equal to the integral over the time of the product $c(t)\,Q$, where Q is the volumetric flow-rate of the carrier liquid, i.e., with help of the above equations:

$$m = \int_t c(t) Q\,dt = Q\int_t c(t)\,dt = Q\,c_0\,\sigma_t\sqrt{2\pi} = Q\frac{S_0}{k}\sigma_t\sqrt{2\pi} \tag{11}$$

where c_0 is the analyte concentration in the detector at time t_0. This amount is a mass or a number of moles if the concentration $c(t)$ is a mass or molar concentration, respectively.

3.2. LOD expressed as an amount of analyte. The concept of detection or quantification limit is a rather complex topic.[25,26] In the following, we consider, as previously done in liquid chromatography[27], that this limit is based on the signal-to-noise ratio and corresponds to the minimum amount of analyte, m_{lim}, that must be injected to provide a peak height $S_{0,\text{lim}}$ equal to an arbitrarily selected multiple, λ, of the noise level, G, defined, as noted above, as the standard deviation of the blank signal, expressed in the same unit as the signal (usually in millivolt). In the study, λ is fixed equal to 3 for the LOD and 10 for the LOQ. Hence the limit corresponds to the minimum analyte concentration, $c_{0,\text{lim}}$, at the peak top equal to:

$$c_{0,\text{lim}} = \frac{\lambda G}{k} \tag{12}$$

The temporal standard deviation, σ_t, is related to the spatial standard deviation, σ_z, when the signal reaches the detector as $\sigma_t = \sigma_z/u$, where u is the mean velocity of the carrier liquid, equal to $Q/(\pi R_c^2)$. Hence, the LOD can be expressed as:

$$m_{LOD} = Q\,\sigma_t \sqrt{2\pi}\,\frac{\lambda G}{k} = \pi R_c^2\,\sigma_z \sqrt{2\pi}\,\frac{\lambda G}{k} \tag{13}$$

As in chromatography, the spatial standard deviation is related to the plate height, H, as $\sigma_z = \sqrt{HL_d}$, where L_d is the length of the capillary from the inlet to the detector. In Taylor conditions[3], the dispersion arising from the nonuniform (parabolic) flow profile dominates the one due to axial diffusion, so the plate height becomes equal to:

$$H = \frac{R_c^2\,u}{24\,D_m} \tag{14}$$

Furthermore, when TDA is performed with a capillary electrophoresis equipment using an *in situ* optical detector, the response factor, which is proportional to the optical path length, *i.e.* equal to the capillary diameter, can be expressed as:

$$k = \kappa R_c \tag{15}$$

where κ is a parameter depending on the analyte attenuation coefficient, but not on the capillary dimensions. Then, the expression of the LOD becomes:

$$m_{LOD} = \pi\sqrt{\frac{\pi}{12}}\, R_c^2 \sqrt{u L_d}\, \frac{\lambda G}{\kappa\sqrt{D_m}} \tag{16}$$

It appears that the LOD expression depends on a numerical constant, on a central group of operating parameters (here R_c , u and L_d) which can be adjusted to optimize the LOD, and on a last fraction which can be considered as a constant for a given analyte and a given detector (assuming that the noise level does not significantly depend on operating conditions).

Alternatively, one may express the LOD as a function of the mean sojourn time, t_0, or of the applied pressure drop, ΔP, along the capillary of length L_c. Noting that $u = L_d/t_0$ and $u = (R_c^2/8\eta)(\Delta P/L_c)$ according to the Poiseuille law, this gives:

$$m_{LOD} = \pi\sqrt{\frac{\pi}{12}}\, \frac{R_c^2 L_d}{\sqrt{t_0}}\, \frac{\lambda G}{\kappa\sqrt{D_m}} = \sqrt{\frac{\pi}{12}}\, \frac{V_d}{\sqrt{t_0}}\, \frac{\lambda G}{\kappa\sqrt{D_m}} \tag{17}$$

where V_d is the volume of the capillary from inlet to detection point. Finally, one gets:

$$m_{LOD} = \frac{\pi}{4}\sqrt{\frac{\pi}{6}}\, R_c^3 \sqrt{\frac{L_d}{L_c}\Delta P}\, \frac{\lambda G}{\kappa\sqrt{\eta D_m}} \tag{18}$$

3.3. LOD expressed as a concentration of analyte in the injected sample. The above expressions give the minimum amount of analyte that must be injected to detect or quantify the analyte by TDA. It may be interesting to express the LOD in terms of the minimum concentration, $c_{inj,LOD}$, of the analyte in the injected sample. The larger the injection volume, the larger the amount of analyte injected in the capillary and the lower the required analyte concentration in the sample, but also the larger the contribution of the injection process to the standard deviation of the peak, which can lead to unacceptable error in the determination of the diffusion coefficient of the analyte by TDA. That is why in TDA, the injection volume V_{inj} is often limited to a fraction, θ, of the capillary volume, V_d, up to the detection point (generally θ is selected equal to 1%):

$$V_{inj} = \theta V_d = \theta \pi R_c^2 L_d \tag{19}$$

Thus, $c_{inj,LOD}$ is related to m_{LOD} as:

$$c_{inj,LOD} = \frac{m_{inj,LOD}}{\theta V_d} = \frac{m_{inj,LOD}}{\theta \pi R_c^2 L_d} \tag{20}$$

Using equations (16)-(18), the minimum concentration can be expressed in terms of the various operating parameters as:

$$c_{inj,LOD} = \sqrt{\frac{\pi}{12}} \sqrt{\frac{u}{L_d}} \frac{\lambda G}{\theta \kappa \sqrt{D_m}} \tag{21}$$

$$c_{inj,LOD} = \sqrt{\frac{\pi}{12}} \sqrt{\frac{1}{t_0}} \frac{\lambda G}{\theta \kappa \sqrt{D_m}} \tag{22}$$

$$c_{inj,LOD} = \frac{1}{4} \sqrt{\frac{\pi}{12}} R_c \sqrt{\frac{\Delta P}{L_d L_c}} \frac{\lambda G}{\theta \kappa \sqrt{\eta D_m}} \tag{23}$$

The central groups of parameters in the right-hand-side term of these equations reflect how the LOD, that is expressed as a concentration in the sample, is affected by any change in the operating parameters.

3.4. Dilution. The amount of analyte injected into the capillary depends on the concentration, c_{inj}, of the analyte in the solution injected and the volume injected, V_{inj}:

$$m_{inj} = c_{inj} V_{inj} \tag{24}$$

Using equations (11), (13) and (24), we can deduce that the dilution factor of the analyte resulting from the migration in the capillary, represented by the ratio of the concentration of the analyte in the sample to the concentration at the top of the detected peak, is equal to:

$$\frac{c_{inj}}{c_0} = \frac{Q \sigma_t \sqrt{2\pi}}{V_{inj}} = \frac{\pi R_c^2 \sigma_z \sqrt{2\pi}}{V_{inj}} \tag{25}$$

3.5. Influence of operating parameters on the LOD expressed in terms of concentration. Simplifying the previous expressions and dropping the numerical factors and the parameters that are considered to be constant (λ, G, κ, η, D_m) in order to better understand the influence of the operating parameters that are easily modifiable (R_c, L_d, u or t_0), equation (25) can be written:

$$c_{inj} \propto \frac{R_c^2 \sigma_z c_0}{V_{inj}} \tag{26}$$

where the sign $\propto$ indicates proportionality rather than equality. In the case where the concentration at the top of the peak, c_0, corresponds to the minimum concentration to allow detection or quantification, the concentration of the injected sample becomes, using equation (12):

$$c_{inj,LOD} \propto \frac{R_c^2 \sigma_z}{k V_{inj}} \tag{27}$$

This relationship is general. The standard deviation σ_z when the peak top passes in front of the detector is equal to $\sqrt{H L_d}$ and, under Taylor conditions using equation (14), σ_z becomes proportional to $R_c \sqrt{u L_d}$, *i.e.* $R_c L_d / \sqrt{t_0}$. Thus, the equation becomes:

$$c_{inj,LOD} \propto \frac{R_c^3 \sqrt{u L_d}}{k V_{inj}} \propto \frac{R_c^3 L_d}{k V_{inj} \sqrt{t_0}} \quad (28)$$

Expression (28) includes the response factor *k* and the volume injected, V_{inj}. Several cases are to be considered depending on the way in which the detection is carried out and the option chosen for V_{inj}.

When the detection takes place in the capillary, the optical path of the detector is proportional to the radius of the capillary (equation (15)), *k* is proportional to R_c, and the LOD becomes:

$$c_{inj,LOD} \propto \frac{R_c^2 \sqrt{u L_d}}{V_{inj}} \propto \frac{R_c^2 L_d}{V_{inj} \sqrt{t_0}} \quad (29)$$

3.6. On-capillary detection at constant V_{inj}/V_d (constant injected percentage). In this case, the injected volume is proportional to the volume of the capillary entering the detector, which keeps the ratio of the length of the injected area to the length of the capillary to the detector constant in order to maintain the contribution of the dispersion injection within acceptable limits. Then, V_{inj} is given by equation (19) with θ constant. Equation (29) becomes:

$$c_{inj,LOD} \propto \sqrt{\frac{u}{L_d}} \propto \frac{1}{\sqrt{t_0}} \quad (30)$$

In that case, *(i)* the LOD does not depend on the capillary radius, *(ii)* the LOD varies as $\sqrt{u}$ at constant L_d or as $1/\sqrt{t_0}$, and therefore only depends on t_0, and (*iii*) the LOD varies as $1/\sqrt{L_d}$ at constant u, since then V_{inj} increases faster than σ_z. These three statements were verified in the experimental part.

4. Results and discussion

4.1. Analysis of different types of vaccine antigens by TDA.

The conditions of validity of TDA depend on the molecular diffusion coefficient (D_m) (see equations (4) and (5)). To be able to size nano-objects from 0.2 to 90 nm in radius[14], while preserving the validity of Taylor conditions, a bare fused silica capillary of 75 cm total length (66.5 cm to the UV detector) × 75 µm i.d. with a mobilization pressure of 40 mbar was used. Moreover, in order to reduce the adsorption of the studied antigens on the bare fused silica capillaries walls, the capillaries were presaturated by performing a preconditioning step consisting of injecting the sample to be analyzed for 2 min at 960 mbar, in order to saturate the possible sites of interactions. The taylorgrams obtained on the four antigens are presented in Figure 1, they were next fitted with the sum of two Gaussians giving access to the average hydrodynamic radius (R_h) of the antigens. The Gaussian fit was performed only on the left part of the elution peaks to avoid any impact of peak tailing on the size measurement. Two-Gaussian fit was required due to the presence of UV-absorbing small molecules in the sample, appearing as the small sharp peak on the top of the signal. The Gaussian fits are presented in Figure SI1 and the average hydrodynamic radii (R_h) obtained are reported in Table 1. DT and TT are the smaller antigens with 3.8 and 5.4 nm respectively, while HBsAg and PRP-T are much larger ones with 13.3 and 33.9 nm respectively. The RSD on the average hydrodynamic radius is typically lower than 5%, as already reported for other polydisperse

samples[28]. The same taylorgrams were fitted by Constrained Regularized Linear Inversion (CRLI) to obtain the size distribution of the antigens presented in Figure 1B. The excellent CRLI fits are presented in Figure SI2. The PRP-T antigen appeared to be highly polydisperse, while the three other antigens have much lower polydispersity index as presented in Figure 1B. The PRP-T antigen appeared to be highly polydisperse with a PI of 0.25, while the 3 other antigens have much lower PI comprised between 0.01 and 0.07 in agreement with the distributions presented in Figure 1B. As in intermediate conclusion, TDA is a simple and straightforward method allowing determining the average hydrodynamic radius and the mass-weighted size distribution of different types of antigens, without calibration.

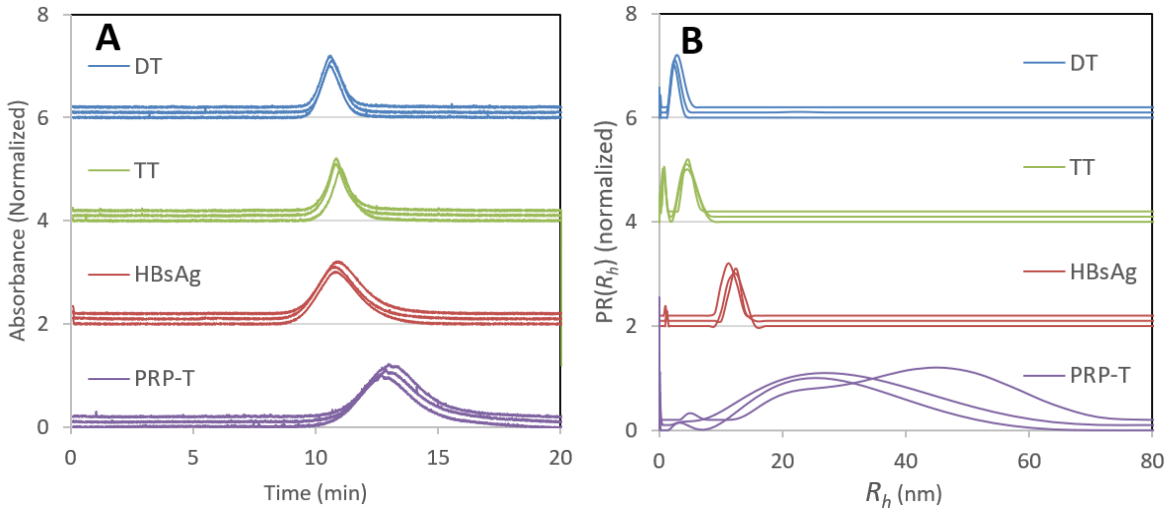

Figure 1: Three repetitions of experimental taylorgrams obtained for four antigens (A), diphtheria toxoid (DT), tetanus toxoid (TT), Hepatitis B surface antigen (HBsAg) and Polyribosyl-ribitol phosphate conjugate (PRP-T), and the corresponding size distributions obtained by CRLI (B). Experimental conditions: bare fused silica capillaries of 75 cm total length (66.5 cm to the UV detector) × 75 µm i.d. Buffers: PBS 10 mM, glycine 200 mM, NaCl 154 mM, pH 6.9, $\eta = 0.9 \times 10^{-3}$ Pa.s for DT and TT ; PBS 10 mM, NaCl 154 mM, pH 7.4, $\eta = 0.9 \times 10^{-3}$ Pa.s for HBsAg, and TRIS 10 mM, sucrose 8% (w/w), pH 7.4, $\eta = 1.1 \times 10^{-3}$ Pa.s [3] for PRP-T. Capillary presaturation: Sample for 10 min at 40 mbar. Capillary preconditioning: water for 2 min at 960 mbar followed by 2 min buffer at 960 mbar. Injections: 20 mbar, 6 s (0.46% of the capillary volume to the detector). Mobilization pressure: 40 mbar. Antigen concentration in sample: 0.4 g/L. UV detection: 215 nm. Temperature: 25°C.

To test the robustness of the R_h values obtained by TDA on a bare fused silica capillary, the experiments were repeated on coated capillaries. Slight adsorption was observed on the right side of the taylorgrams on the bare fused silica capillaries, as can be seen on the Gaussian fit in Figure SI1. Thus, neutral hydroxypropylcellulose (HPC) coated capillaries were tested. The taylorgrams obtained are presented in Figure SI3A. A bare fused silica capillary of lower I.D. (50 µm) was also tested to verify how robust the R_h values are regarding a change on operating conditions. The taylorgrams obtained are presented in Figure SI3B. The R_h results are reported in Table 1. No major difference was observed concerning the values obtained on the three capillaries, which confirms the robustness of the results, in good agreement with a previous study showing that all TDA experiments should lead to similar results as long as the operating conditions verify the conditions of validity of the TDA method.[24] It is worth noting that the presence of significant adsorption on the capillary wall would impact the R_h by increasing the apparent value due to additional peak dispersion. As many different combinations of operating parameters (capillary diameter and length, mobilizing pressure) allow to fulfill Taylor conditions of validity, it is sometimes difficult to choose the initial parameters to develop a new TDA method, especially in view to improve the limits of detection (LOD) / quantification (LOQ).

Table 1: Average hydrodynamic radii (R_h) of the four antigens studied obtained by Gaussian fit of the TDA elution profiles. The standard deviation was calculated over three repetitions. Experimental conditions: the same as in Figure 1.

	Average R_h (nm)			
	DT	TT	HBsAg	PRP-T
Fused Silica 75 µm	3.8 ± 0.2	5.4 ± 0.3	13.3 ± 0.3	33.9 ± 0.3
HPC 75 µm	3.7 ± 0.1	5.4 ± 0.3	12.8 ± 0.2	34.2 ± 1.5
Fused Silica 50 µm	3.9 ± 0.1	5.5 ± 0.1	12.2 ± 0.5	35.2 ± 0.8

4.2. Optimization of the limit of detection (LOD). The LOD is a limiting factor in vaccines analysis as vaccine antigens are often present at very low concentrations in formulations. The possibility of finding a specific set of operating parameters that will allow to lower the LOD by TDA is thus desirable. This question is very general and may be also relevant for any other solute / sample. First, the impact of the internal diameter of the capillary on the LOD was studied. The same six solutions (0.32, 0.16, 0.08, 0.04, 0.02 and 0.01 g/L) of HBsAg antigen in PBS buffer were analyzed by TDA on three capillaries of different internal diameters using the same linear velocity of the eluent, the same capillary length and at constant V_{inj}/V_d (constant injected length) (Figure 2A). The calibration curves allowing the determination of the LOD are presented in Figure 2B. The different conditions tested and the LOD obtained are summarized in Table 2. It appeared that the LOD did not significantly depend on the diameter of the capillaries, thus confirming the theoretical result derived from equation (30). The larger optical path in larger diameter capillaries is compensated by a higher dispersion of the molecules in these capillaries. Thus, taking a capillary with a larger diameter did not provide better sensitivity in TDA. Therefore, using a 50 µm capillary is generally recommended, as it consumes less product. However, the diameter of the capillary may also have an impact on the adsorption of the molecules on the capillary wall, however no visible impact of the capillary diameter on the adsorption was observed in this study.

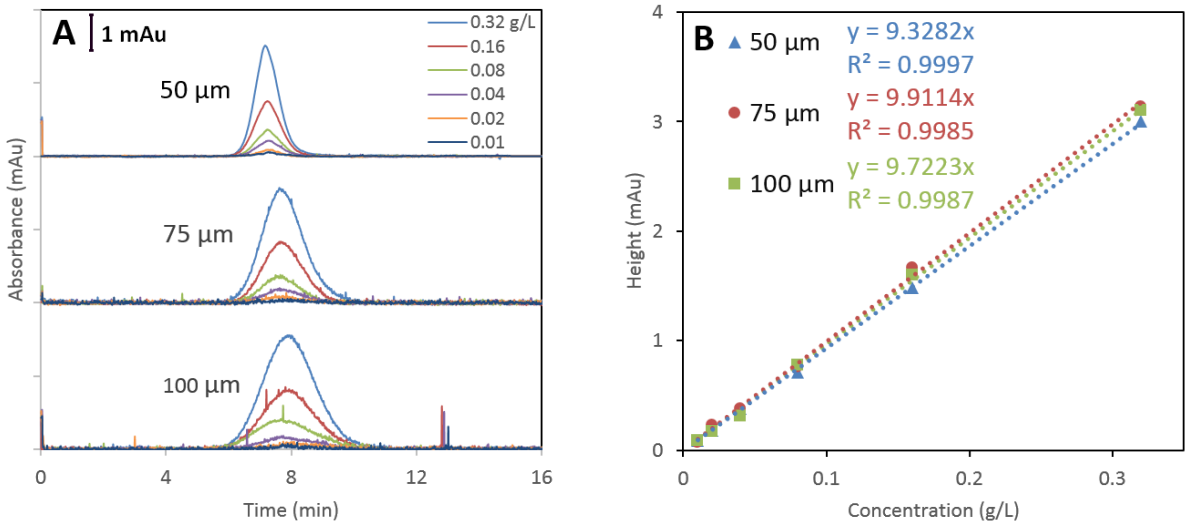

Figure 2: Impact of the capillary internal diameter (i.d.) on the limit of detection (LOD). Experimental taylorgrams obtained on three capillaries of different internal diameters (i.d.) 50 µm, 75 µm and 100 µm (A) and the associated calibration curves representing the height of the obtained peaks as a function of the concentration of the analyzed samples. Experimental conditions: bare fused silica capillaries of 50 cm total length (41.5 cm to the UV detector). Sample: Hepatitis B surface antigen (HBsAg). Buffer: PBS 10 mM, NaCl 154 mM, pH 7.4, $\eta = 0.9 \times 10^{-3}$ Pa.s. Capillary presaturation: Sample for 10 min at 40 mbar. Capillary preconditioning: water for 2 min at 960 mbar followed by 2 min buffer at 960 mbar. Injections: 20 mbar 6 s (0.5% of the capillary volume to the detector) on 50 µm i.d. capillary, 18 mbar 3s (0.5% of the capillary volume to the detector) on 75 µm i.d. capillary, 10 mbar 3s (0.5% of the capillary volume to the detector) on 100 µm i.d. capillary. Mobilization pressure: 50 mbar on 50 µm i.d. capillary, 22 mbar on 75 µm i.d. capillary, 12.5 mbar on 100 µm i.d. capillary. UV detection: 215 nm. Temperature: 25°C.

Table 2: Influence of the operating conditions on the LOD or LOQ of HBsAg antigen.

	Capillary diameter (µm)	Mobilization pressure (mbar)	Total capillary length (cm)	Injection[a]	LOD (g/L)	LOQ (g/L)
Figure 2: Impact of capillary internal diameter	**50**	50	50	20 mbar 6s (0.5%)	0.021	0.070
	75	22	50	18 mbar 3s (0.5%)	0.018	0.061
	100	12.5	50	10 mbar 3s (0.5%)	0.019	0.062
Figure 3: Impact of mobilization pressure	50	**50**	50	20 mbar 6s (0.5%)	0.021	0.070
	50	**30**	50	20 mbar 6s (0.5%)	0.016	0.052
	50	**20**	50	20 mbar 6s (0.5%)	0.013	0.044
	50	**10**	50	20 mbar 6s (0.5%)	0.010	0.033
Figure 4: Impact of capillary length	50	22	**40**	12 mbar 6s (0.5%)	0.019	0.063
	50	28	**50**	20 mbar 6s (0.5%)	0.016	0.054
	50	39	**70**	41 mbar 6s (0.5%)	0.014	0.047
	50	50	**90**	42 mbar 10s (0.5%)	0.013	0.042

[a] The percentage of the injected volume relative to the detection volume is given in parenthesis.

In a second time, the impact of the pressure (and thus of the average elution time) on the LOD was studied by TDA at constant V_{inj}/V_d (constant injected length). Different mobilization pressures of 10, 20, 30 and 50 mbar were tested on a same capillary (50 µm × 50 cm bare fused silica capillary, Figure 3A). The calibration curves allowing the determination of the LOD are presented in Figure 3B and the linear function representing the limit of detection (LOD) as a function of $1/\sqrt{t_0}$ is presented in Figure 3C, in good agreement with eq. (28). The lower the pressure, the higher t_0, the more sensitive the method to the detriment of the analysis time. The right balance between the duration of analysis and the sensitivity must therefore be found.

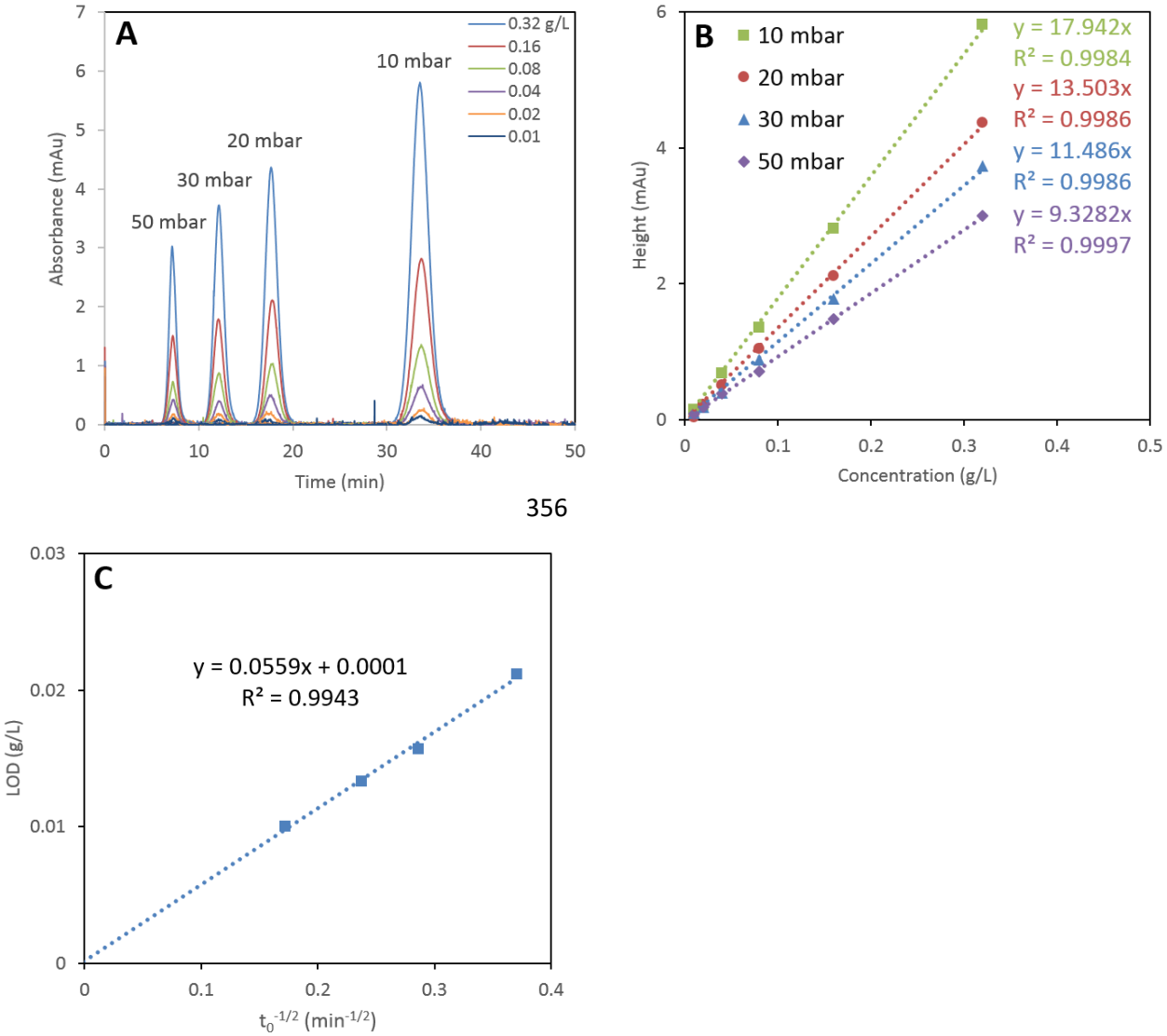

Figure 3: Impact of the mobilization pressure on the limit of detection (LOD) of HBsAg antigen. Experimental taylorgrams obtained on a same capillary using different mobilization pressures 50, 30, 20 and 10 mbar (A), the associated calibration curves representing the height of the obtained peaks as a function of the concentration of the analyzed samples (B) and the linear correlation of the limit of detection (LOD) as a function $1/\sqrt{t_0}$ (C). Experimental conditions: bare fused silica capillaries of 50 cm total length (41.5 cm to the UV detector) × 50 µm i.d. Injections: 20 mbar, 6 s (0.5% of the capillary volume to the detector). Other experimental conditions: as in Figure 2.

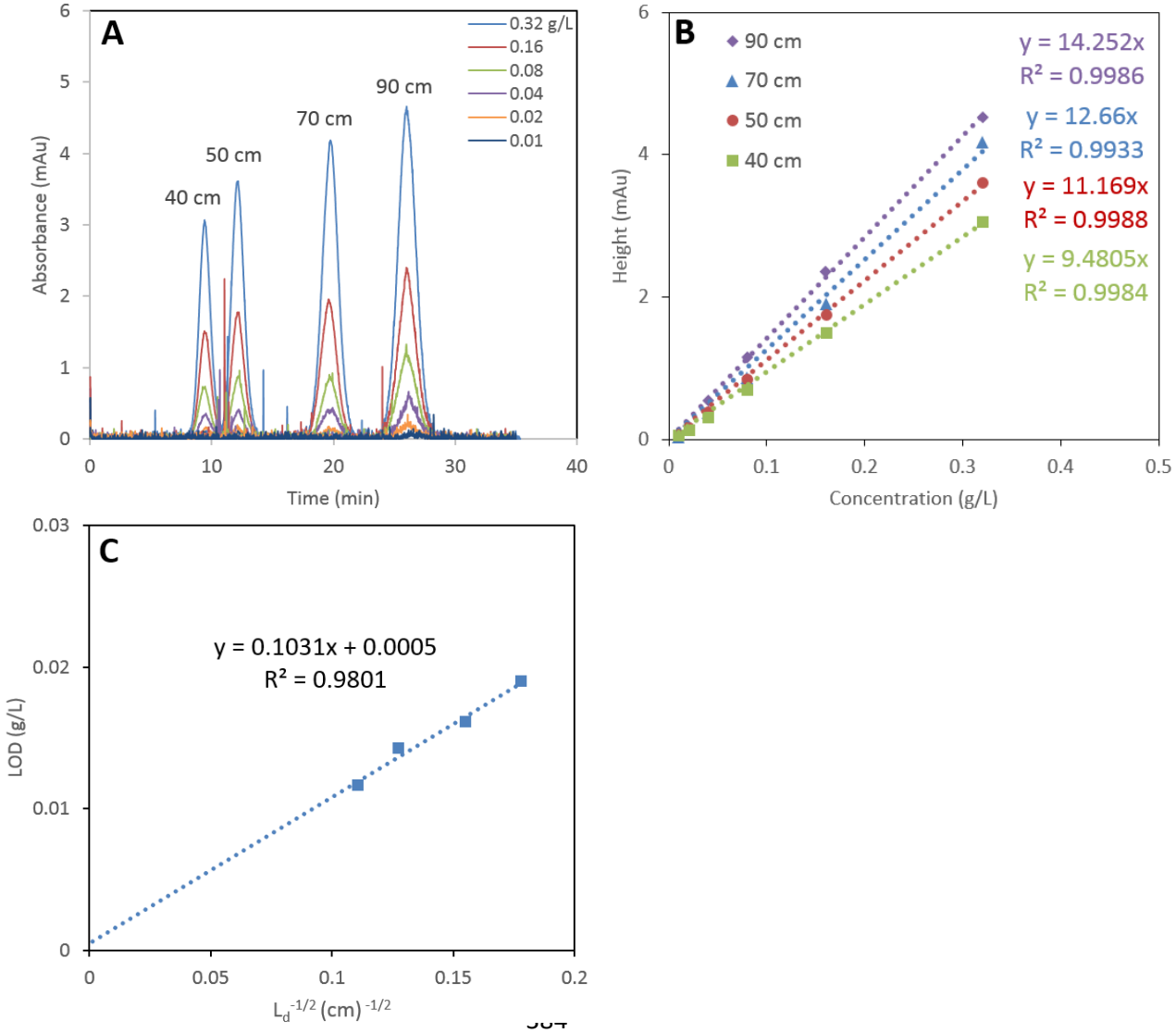

Figure 4: Impact of the capillary length on the limit of detection (LOD) of HBsAg antigen. Experimental taylorgrams obtained on four capillaries of different total lengths 40, 50, 70 and 90 cm (A), the associated calibration curves representing the height of the obtained peaks as a function of the concentration of the analyzed samples (B) and the linear correlation representing the limit of detection (LOD) as a function of $1/\sqrt{L_d}$ (C). Experimental conditions: bare fused silica capillaries of 50 µm i.d. The detection window is located 8.5 cm from the capillary end (L_c=L_d+8.5 in cm). Injections: 12 mbar 6 s (0.49 % % of the capillary volume to the detector) on the 40 cm capillary, 20 mbar 6 s (0.49 % of the capillary volume to the detector) on the 50 cm capillary, 41 mbar 6 s (0.49 % of the capillary volume to the detector) on the 70 cm capillary and 42 mbar 10 s (0.49 % of the capillary volume to the detector) on the 90 cm capillary. Mobilization pressure: 22 mbar on the 40 cm capillary, 28 mbar on the 50 cm capillary, 39 mbar on the 70 cm capillary and 50 mbar on the 90 cm capillary. Other experimental conditions: as in Figure 2.

Finally, the impact of the capillary length on the LOD was studied. Different total capillary lengths of 40, 50, 70 and 90 cm were studied by TDA at constant linear velocity of the eluent and at

constant V_{inj}/V_d (Figure 4A, $L_c=L_d+8.5$ in cm). Note that constant V_{inj}/V_d means increasing injected length on capillaries of increasing total length. The calibration curves allowing the determination of the LOD are presented in Figure 4B and the linear function representing the LOD as a function of $1/\sqrt{L_d}$ are presented in Figure 4C. At constant V_{inj}/V_d, the longer the capillary the lower the LOD. As for the influence of the mobilization pressure at constant V_{inj}/V_d, the LOD increased as the analysis time lengthened scaling as $1/\sqrt{t_0}$. A 60 cm capillary may be a good starting choice for the development of a new TDA method.

Conclusions

This work first showed that TDA is a suitable method for the determination of the average R_h, the polydispersity and the size distribution of different types of vaccine antigens such as toxoids, glycoconjugates and subviral particles, as far as the size of the antigen remains in the typical sizing range of TDA (i.e. from 0.1 to 300 nm). Moreover, the results obtained were consistent whatever the diameter and the capillary coating used, showing the robustness of the TDA methodology. Since the limit of detection (LOD) is a limiting factor of the analytical methods for vaccine antigen characterization due to their low concentration in vaccine formulations, the impact of operational parameters on the LOD was investigated. A very good correlation between theory and experiment was observed. It has been shown that at constant injected percentage relative to the detection volume, the LOD did not depend on the capillary radius. Then, the impact of the mobilization pressure on the LOD was studied on a same capillary at constant linear velocity of the eluent. It appeared that the LOD varies as $1/\sqrt{t_0}$ as predicted by the theory. The lower the pressure, the more sensitive the TDA method, but to the detriment of the analysis time. It is often beneficial to start the development of a method with a not too low mobilization pressure to be able to do a large number of analyzes in limited time and decrease the pressure afterwards to increase

the LOD as needed. Finally, the impact of the length of the capillary was studied, the LOD varies as $1/\sqrt{L_d}$ at constant V_{inj}/V_d and constant u. Taking a longer capillary therefore allows to reduce the LOD but the analysis time is also longer. Last but not least, to decrease the LOD, it is also possible to slightly adjust the percentage injected by approaching 1% V_d. Following these results, starting with a 50 µm i.d. × 60 cm total length capillary and applying 50 mbar mobilization pressure is recommended to analyze molecules from 0.5 to 125 nm remaining under TDA validity conditions. Typical RSD about 1 to 5% (3% in average) were obtained for the R_h determination of vaccine antigen at concentrations (0.4 g/L) well above the LOQ. The conclusion from this work about how improving the LOD in TDA is very general and can be of course applied to the analysis of any sample in TDA.

Ackowledgments

This work was partly funded by Sanofi under a Cooperative Research and Development Agreement with the University of Montpellier and the CNRS.

Declaration of competing interest

The authors declare no conflict of interest. Camille Malburet, Jean-François Cotte and Jérôme Thiebaud are Sanofi employees and may hold shares or stocks in the company.

Supporting Information.

Gaussian fits of the TDA elution profiles allowing to calculate the average hydrodynamic radii. CRLI fits of the TDA elution profiles allowing to calculate the size distributions. Experimental taylorgrams of four antigens obtained of different capillaries.

References

[1] G. I. Taylor, Dispersion of Soluble Matter in Solvent Flowing Slowly through a Tube, Proc. R. Soc. Lond. 219 1137, (1953), 186–203. https://doi.org/10.1098/rspa.1953.0139.

[2] R. Aris, On the Dispersion of a Solute in a Fluid Flowing through a Tube, Proc. R. Soc. Lond. 235 1200, (1956), 67–77. https://doi.org/10.1098/rspa.1956.0065.

[3] G. I. Taylor, Conditions under Which Dispersion of a Solute in a Stream of Solvent Can Be Used to Measure Molecular Diffusion, Proc. R. Soc. Lond. 225, 1163, (1954), 473–477. https://doi.org/10.1098/rspa.1954.0216.

[4] W. E. Price, Theory of the Taylor Dispersion Technique for Three-Component-System Diffusion Measurements, J. Chem. Soc. Faraday Trans. 84, 7, (1988), 2431–2439. https://doi.org/10.1039/F19888402431.

[5] H. Cottet, J.-P. Biron, M. Martin, Taylor Dispersion Analysis of Mixtures, Anal. Chem. 79, 23, (2007), 9066–9073. https://doi.org/10.1021/ac071018w.

[6] H. Cottet, J.-P. Biron, L. Cipelletti, R. Matmour, M. Martin, Determination of Individual Diffusion Coefficients in Evolving Binary Mixtures by Taylor Dispersion Analysis: Application to the Monitoring of Polymer Reaction, Anal. Chem. 82, 5, (2010), 1793–1802. https://doi.org/10.1021/ac902397x.

[7] L. Cipelletti, J.-P. Biron, M. Martin, H. Cottet, Measuring Arbitrary Diffusion Coefficient Distributions of Nano-Objects by Taylor Dispersion Analysis, Anal. Chem. 87, 16, (2015), 8489–8496. https://doi.org/10.1021/acs.analchem.5b02053.

[8] W. L. Hulse, R. T. Forbes, A Nanolitre Method to Determine the Hydrodynamic Radius of Proteins and Small Molecules by Taylor Dispersion Analysis, Int. J. Pharm. 411, 1, (2011), 64–68. https://doi.org/10.1016/j.ijpharm.2011.03.040.

[9] J. Hong, H. Wu, R. Zhang, M. He, W. Xu, The Coupling of Taylor Dispersion Analysis and Mass Spectrometry to Differentiate Protein Conformations, Anal. Chem. 92, 7, (2020), 5200–5206. https://doi.org/10.1021/acs.analchem.9b05745.

[10] J.-P. Biron, F. Bonfils, L. Cipelletti, H. Cottet, Size-Characterization of Natural and Synthetic Polyisoprenes by Taylor Dispersion Analysis, Polym. Test. 66, (2018), 244–250. https://doi.org/10.1016/j.polymertesting.2018.01.017.

[11] U. Franzen, C. Vermehren, H. Jensen, J. Østergaard, Physicochemical Characterization of a PEGylated Liposomal Drug Formulation Using Capillary Electrophoresis, Electrophoresis. 32, 6-7, (2011), 738–748. https://doi.org/10.1002/elps.201000552.

[12) J. Chamieh, V. Jannin, F. Demarne, H. Cottet, Hydrodynamic Size Characterization of a Self-Emulsifying Lipid Pharmaceutical Excipient by Taylor Dispersion Analysis with Fluorescent Detection, Int. J. Pharm. 513, 1, (2016), 262–269. https://doi.org/10.1016/j.ijpharm.2016.09.016.

[13] J. Chamieh, H. Merdassi, J.-C. Rossi, V. Jannin, F. Demarne, H. Cottet, Size Characterization of Lipid-Based Self-Emulsifying Pharmaceutical Excipients during Lipolysis Using Taylor Dispersion Analysis with Fluorescence Detection, Int. J. Pharm. 537, 1, (2018), 94–101. https://doi.org/10.1016/j.ijpharm.2017.12.032.

[14] J. Chamieh, L. Leclercq, M. Martin, S. Slaoui, H. Jensen, J. Østergaard, H. Cottet, Limits in Size of Taylor Dispersion Analysis: Representation of the Different Hydrodynamic Regimes and Application to the Size-Characterization of Cubosomes, Anal. Chem. 89, 24, (2017), 13487–13493. https://doi.org/10.1021/acs.analchem.7b03806.

[15] C. Malburet, L. Leclercq, J.-F. Cotte, J. Thiebaud, S. Marco, M.-C. Nicolaï, H. Cottet, Antigen-Adjuvant Interactions in Vaccines by Taylor Dispersion Analysis: Size Characterization and Binding Parameters, Anal. Chem. 93, 16, (2021), 6508–6515. https://doi.org/10.1021/acs.analchem.1c00420.
[16] C. Malburet, L. Leclercq, J.-F. Cotte, J. Thiebaud, E. Bazin, M. Garinot, H. Cottet, Size and Charge Characterization of Lipid Nanoparticles for MRNA Vaccines, Anal. Chem. 94, 11, (2022), 4677–4685. https://doi.org/10.1021/acs.analchem.1c04778.
[17] B. Greenwood, The Contribution of Vaccination to Global Health: Past, Present and Future, Phil. Trans. R. Soc. B. 369 1645, 20130433, (2014), 1-9. https://doi.org/10.1098/rstb.2013.0433.
[18] I. Hajj Hussein, N. Chams, S. Chams, S. El Sayegh, R. Badran, M. Raad, A. Gerges-Geagea, A. Leone, A. Jurjus, Vaccines Through Centuries: Major Cornerstones of Global Health, Front. Public Health. 3, 269, (2015), 1-16. https://doi.org/10.3389/fpubh.2015.00269.
[19] F. E. Andre, R. Booy, H. L. Bock, J. Clemens, S. K. Datta, T. J. John, B. W. Lee, S. Lolekha, H. Peltola, T. A. Ruff, M. Santosham, H. J. Schmitt, Vaccination Greatly Reduces Disease, Disability, Death and Inequity Worldwide, Bull. World Health Organ. 86, 2, (2008), 140–146. https://doi.org/10.2471/blt.07.040089.
[20] D. M. Morens, A. S. Fauci, Emerging Pandemic Diseases: How We Got to COVID-19, Cell. 182, 5, (2020), 1077–1092. https://doi.org/10.1016/j.cell.2020.08.021.
[21] M. Saxena, S. H. Van Der Burg, C. J. M. Melief, N. Bhardwaj, Therapeutic Cancer Vaccines, Nat. Rev. Cancer. 21, 6, (2021), 360–378. https://doi.org/10.1038/s41568-021-00346-0.
[22] C. Janus, Vaccines for Alzheimer's Disease: How Close Are We? CNS Drug Rev. 17, 7, (2003), 457–474. https://doi.org/10.2165/00023210-200317070-00001.
[23] Y. Shen, R. D. Smith, High-Resolution Capillary Isoelectric Focusing of Proteins Using Highly Hydrophilic-Substituted Cellulose-Coated Capillaries, J. Microcolumn Sep. 12, 3, (2000), 135–141. https://doi.org/10.1002/(SICI)1520-667X(2000)12:3<135::AID-MCS2>3.0.CO;2-5.
[24] H. Cottet, J.-P. Biron, M. Martin, On the Optimization of Operating Conditions for Taylor Dispersion Analysis of Mixtures. Analyst 139, 14, (2014), 3552–3562. https://doi.org/10.1039/c4an00192c.
[25] R. Boqué, Y. Vander Heyden, The Limit of Detection, LCGC Europe. (2009), 22, 2, 82–85.
[26] A. Hubaux, G. Vos, Decision and detection limits for calibration curves, Anal. Chem. 42, 8, (1970), 849-855. https://doi.org/10.1021/ac60290a013
[27] B. L. Karger, M. Martin, G. Guiochon, Role of Column Parameters and Injection Volume on Detection Limits in Liquid Chromatography. Anal. Chem. 46, 12, (1974), 1640–1647. https://doi.org/10.1021/ac60348a053.
[28] J. Chamieh, H. Cottet, Comparison of Single and Double Detection Points Taylor Dispersion Analysis for Monodisperse and Polydisperse Samples, Journal of Chromatography A. 1241, (2012), 123–127. https://doi.org/10.1016/j.chroma.2012.03.095.